Journal of Innate Immunity

Research Article

J Innate Immun 2022;14:532–542
DOI: 10.1159/000522231

Received: April 10, 2021
Accepted: January 13, 2022
Published online: May 19, 2022

miR-142-5p Encapsulated by Serum-Derived Extracellular Vesicles Protects against Acute Lung Injury in Septic Rats following Remote Ischemic Preconditioning via the PTEN/PI3K/Akt Axis

Wenliang Zhu[a] Xiaopei Huang[a] Shi Qiu[a] Lingxiao Feng[a] Yue Wu[b] Huanzhang Shao[a]

[a]Department of Critical Care Medicine, Henan Key Laboratory for Critical Care Medicine, Zhengzhou Key Laboratory for Critical Care Medicine, Henan Provincial People's Hospital, Zhengzhou University People's Hospital, Zhengzhou, PR China; [b]Digestive System Department, Henan Provincial People's Hospital, Zhengzhou University People's Hospital, Zhengzhou, PR China

Keywords
Acute lung injury · Sepsis · Remote ischemic preconditioning · Extracellular vesicles · miR-142-5p · Phosphatase and tensin homologue deleted on chromosome 10

Abstract
This study intends to investigate the effects of miR-142-5p encapsulated by serum-derived extracellular vesicles (EVs) on septic acute lung injury (ALI) following remote ischemic preconditioning (RIPC) through a PTEN-involved mechanism. ALI was induced in rats by lipopolysaccharide (LPS) injection, 24 h before which RIPC was performed via the left lower limb. Next, the binding affinity between miR-142-5p and PTEN was identified. EVs were isolated from serum and injected into rats. The morphology of lung tissues, pulmonary edema, and inflammatory cell infiltration into lung tissues were then assessed, and TNF-α and IL-6 levels in serum and lung tissues were measured. The results indicated that RIPC could attenuate ALI in sepsis. miR-142-5p expression was increased in serum, lung tissues, and serum-derived EVs of ALI rats following RIPC. miR-142-5p could target PTEN to activate the PI3K/Akt signaling pathway. miR-142-5p shuttled by serum-derived EVs reduced pulmonary edema, neutrophil infiltration, and TNF-α and IL-6 levels, thus alleviating ALI in LPS-induced septic rats upon RIPC. Collectively, serum-derived EVs-loaded miR-142-5p downregulated PTEN and activated PI3K/Akt to inhibit ALI in sepsis following RIPC, thus highlighting potential therapeutic molecular targets against ALI in sepsis.

Introduction

Sepsis, as a life-threatening clinical syndrome, is characterized by organ dysfunction resulting from the dysregulated response to infection [1]. Organ dysfunctions occur frequently in patients with sepsis, and the lungs are particularly vulnerable; approximately 50% of acute lung injury (ALI) or acute respiratory distress syndrome arises due to sepsis [2]. In recent years, remote ischemic preconditioning (RIPC) has been found to be beneficial, comprising stimulation induced by transient ischemia-reperfusion of distal tissue, which was initially used for cardiac protection [3]. Studies have also demonstrated that RIPC is a practical, clinically applicable method for protecting against the acute

Karger@karger.com
www.karger.com/jin

Correspondence to:
Huanzhang Shao, zhuwenliang2020@126.com

kidney injury and heart injury [4, 5]. RIPC is also confirmed to ameliorate lipopolysaccharide (LPS)-induced ALI in septic mice [6]. However, the mechanisms by which RIPC modulates sepsis-induced ALI remain to be established.

Extracellular vesicles (EVs) have become an important cell-cell communication entity in physiological and pathological processes acting as carriers of many biomolecules, including microRNAs (miRNAs), which are involved in many biological processes inherent to inflammatory diseases, including lung injury in acute respiratory distress syndrome [7]. Existing literature has confirmed that EVs delivering miRNA can mitigate ALI [8]. miRNAs are highly conserved small noncoding RNAs, 21–23 nucleotides in length, and can regulate relevant genes by inhibiting translation or inducing RNA degradation [9]. miRNAs serve as critical regulators of cell proliferation, apoptosis, and inflammation [10]. Growing evidence has demonstrated the effects of miRNAs on inflammatory response in sepsis-induced ALI [11, 12]. miR-142-5p is one of the two small single-chain molecules formed by the precursor of miR-142 during the maturation [13]. Downregulated expression of miR-142-5p has been suggested in sepsis [14], whereas the involvement of miR-142-5p in sepsis-induced ALI remains to be elucidated.

Of interest, phosphatase and tensin homologue deleted on chromosome 10 (PTEN) is identified to be a direct target gene of miR-142-5p [15]. PTEN, as a dual-function lipid and protein phosphatase, has emerged as a tumor suppressor gene [16]. PTEN can also regulate innate and adaptive immunity during lung inflammation [17]. A role of PTEN in sepsis-induced ALI has also been demonstrated [18]. However, the mechanisms by which serum-derived EVs communication affects ALI in sepsis following RIPC remain unclear; specifically those involving the putative interplay between miR-142-5p, PTEN, and PI3K/Akt have not been explored. Such knowledge could support a notion that serum-derived EVs may be of significance to ALI in sepsis after RIPC. Hence, herein we hypothesized that the transfer of miR-142-5p via serum-derived EVs might alter ALI in sepsis following RIPC, which may associate with PTEN and PI3K/Akt.

Materials and Methods

Animal Acclimatization

Two-month-old male Sprague-Dawley rats, weighing 160–185 g, were provided by Shanghai Model Organisms Center (Shanghai, China). All rats were housed at 24 ± 1°C under a humidity of 65% and a 12-h light/dark cycle, with free access to food and water, for a period of 1 week.

RIPC in Rats

After overnight fasting, rats were anesthetized intraperitoneally with anesthetic cocktail (1.8 mL/kg) containing fentanyl (0.0166 mg; Abbot Laboratories, Abbott Park, IL, USA) and midazolam (1.66 mg; La Roche Ltd., Basel, Switzerland) per milliliter. Anesthesia was maintained throughout surgery using repeated doses of anesthetics. Though placing a 1-cm-wide, 30-cm-long rubber band tourniquet across the upper thigh of the left lower limb, lower limb ischemia lasted for 10 min (3 cycles). The cessation of arterial blood flow was confirmed by a laser flow meter (Laser Flo BPM2; Vasamedics, Minneapolis, MN, USA), which was put on the limb distal to the tourniquet.

LPS-Induced Septic ALI Rat Model

To establish LPS-induced septic ALI rat models, rats were randomly allocated into the following 4 groups (n = 16): (1) saline group (rats were injected with the same amount of normal saline); (2) LPS group (rats were injected with *Escherichia coli* O111: B4, L2880 [5 mg/kg; Sigma-Aldrich, St. Louis, MO, USA] dissolved in 1 M 0.9% sodium chloride via tail vein); and (3) RIPC + LPS group (RIPC was performed in the left lower limb of rats 24 h before LPS injection). After LPS stimulation, 10 rats in each group were observed for 7 days to evaluate the survival rate. Survival of these animals was observed by a blinded researcher. In addition, after blood collection, 6 rats in each group were euthanized 6 h after LPS treatment, and lung tissue was obtained for subsequent analysis. The EVs (70 μg) or the NC PBS was injected through vena jugularis externa into rats of the corresponding group 12 h after the establishment of ALI [19, 20].

Hematoxylin and Eosin Staining

Lung tissues were excised and prepared into paraffin-embedded sections of a thickness of 4–6 mm. After staining with hematoxylin and eosin (HE), pathological changes were observed utilizing a light microscope (BXFM; Olympus, Tokyo, Japan). The lung injury was scored by assessing inflammatory cell infiltration in alveolar congestion or airspace, vessel wall, hemorrhage, alveolar wall thickness, and hyaline membrane formation, based on which scores of 0, 1, 2, 3 and 4 indicated no, mild, moderate, severe, and very severe damage, respectively [9].

Lung Wet/Dry Ratio

Severity of pulmonary edema was assessed through measurement of lung wet/dry ratio. Briefly, the right lung was isolated and weighed, followed by drying at 80°C for 48 h and measurement of dry weight.

Myeloperoxidase Evaluation

Lung tissues were homogenized with reaction buffer (1/9 wt/vol), and a myeloperoxidase (MPO) activity detection kit (Nanjing Jiancheng Bioengineering Institute, China) was utilized. MPO activity, an indicator for inflammatory cell infiltration, was characterized as MPO/mg unit protein in the homogenate utilizing a DC protein assay (Bio-Rad, Hercules, CA, USA) after the detergent solubilization of MPO.

ELISA

Rats were anesthetized with an anesthetic cocktail (1.8 mL/kg) to collect blood sample. The blood was centrifuged (2,000 rpm, 4°C) for 10 min, and lung tissue homogenates were centrifuged

(14,000 rpm, 4°C) for 10 min. Collected supernatants were both subjected to ELISA determination of proinflammatory cytokines (IL-1β, IL-6, and TNF-α) utilizing corresponding ELISA kits (Bio Legend, San Diego, CA, USA). The optical density at 450 nm was quantified with the use of a microplate reader (MultiskanMK3; Thermo Scientific, Waltham, MA, USA).

Preparation and Administration of miR-142-5p

miR-142-5p was synthetized by VBC Biotech (Vienna, Austria). The mature miR-142-5p and control oligonucleotides were dissolved in PBS. LPS-challenged Sprague-Dawley rats were injected with miR-142-5p or miR-control (200 μL, 8 mg/kg), referred to as miR-control + LPS and miR-142-5p + LPS groups (6 rats in each group), respectively. Specifically, the rats were injected before LPS treatment with miR-142-5p or miR-control, 8 mg/kg once a day for 3 days. LPS or saline induction was performed on the second day after the final injection.

Isolation and Identification of EVs from Serum

The blood collected from rat jugular vein was centrifuged (3,000 *g*) for 25 min to collect the serum. After 30-min centrifugation of the serum (3,000 *g*, 4°C), the supernatant diluted with PBS (pH 7.4) was subjected to another 30-min centrifugation (10,000 *g*, 4°C). The supernatant harvested was filtered through a 0.22-mm filter (Millipore), followed by 2-h centrifugation (200,000 *g*).

For EV purification, the pellets were centrifuged at (200,000 *g*, 4°C) for 1 h, and the EV-contained pellets were resuspended in filtrated PBS. Isolated EVs were analyzed using electron microscopy and nanoparticle tracking analysis. Protein markers such as CD63 and CD81 were quantified by flow cytometry, with PBS as the control.

The isolated serum EVs were fixed in 2% paraformaldehyde, loaded onto a Formvar carbon coated grid, and then allowed to stand for 15 min. After that, the samples were negatively stained for 5 min with uranyl oxalate, which were subsequently viewed utilizing a Hitachi H-600 transmission electron microscope (Hitachi, Schaumburg, IL, USA).

The EVs were labeled with PKH67 green fluorescence (Sigma; MINI67). After 15-min centrifugation (14,000 *g*) to remove residual dye, EVs were resuspended in 200 μL PBS. After LPS induction, the rats were injected with serum-derived EVs (200 μg) via the tail vein. The control rats were injected with PBS. Prepared sections of lung tissues were stained with DAPI for 10 min and observed with fluorescence microscope (AX70; Olympus).

Bioinformatics Analysis

A sepsis-induced ALI-related miRNA expression dataset (GSE111241) was downloaded from the GEO database, which included 3 LPS-induced ALI rat model samples and 3 normal control samples. Differentially expressed genes in sepsis-induced ALI were identified using the "limma" package in R language, with $p < 0.05$ and $|\log FC| > 1$ set as the threshold.

Isolation and Quantification of RNA

TRIzol reagent (Invitrogen, Carlsbad, CA, USA) was applied to extract total RNA from tissues or EVs. The quality of RNA was determined by RNA gel electrophoresis. Total RNA (5 μg) was reversely transcribed into cDNA utilizing a cDNA synthesis kit (K1622; Fermentas, Ontario, CA, USA); and the poly(A) tailing method was applied to synthesize cDNA from miRNA with the use of the microRNA reverse transcription kit (EZB-miRT2; EZBioscience, Roseville, MN, USA).

Reverse transcription quantitative polymerase chain reaction (RT-qPCR) was conducted utilizing the SYBR Green Plus Kit (Roche Applied Science, Mannheim, Germany) on an ABI 7500 instrument (Applied Biosystems, Foster City, CA, USA). Three replicates were set for RT-qPCR. U6 was used as an internal reference. The $2^{-\Delta\Delta Ct}$ method was used to quantify the relative mRNA expression. The primer sequences of genes are listed in online supplementary Table 1 (for all online suppl. material, see www.karger.com/doi/10.1159/000522231).

Western Blot Analysis

The total protein was extracted from EVs or lung tissues using RIPA buffer (BioSharp, Beijing, China), followed by the measurement of protein concentration with the use of a BCA kit (Thermo Fisher Scientific, Rockford, IL, USA). The protein was separated by sodium dodecyl sulfate-polyacrylamide gel electrophoresis and electrotransferred onto a PVDF membrane, which was subsequently incubated with the primary antibodies overnight at 4°C. Afterward, the membrane was incubated with the horseradish peroxidase-labeled secondary antibody. The ImageQuant LAS4000 mini (GE Healthcare, Piscataway, NJ, USA) was used to visualize the membrane. The primary antibodies against PTEN (ab267787, 1:1,000), p-AKT (ser473, ab81283, 1:5,000), and AKT (ab8805, 1:500) were purchased from Abcam (Cambridge, UK).

Dual-Luciferase Reporter Gene Assay

Wild-type and mutant 3′-untranslated region of PTEN were cloned into the pGL3 vector (Promega, Madison, WI, USA). Cells were seeded into 24-well plates (5×10^5 cells/well). Constructed wild-type and mutant reporter plasmids were then cotransfected with miR-142-5p mimic or NC-mimic (GenePharma, Shanghai, China) into HEK293T cells (American Type Culture Collection, Manassas, VA, USA) utilizing Lipofectamine 3000 transfection reagent (Invitrogen). The luciferase activity was determined 24 h later with the use of a Dual-Luciferase® Reporter Assay System (Promega).

Statistical Analysis

Data analysis was performed using SPSS 18.0 software (SPSS Inc., Chicago, IL, USA). All quantitative data were summarized as mean ± standard deviation. An unpaired *t* test was used for the comparison of the data between 2 groups. Comparisons of the data from multiple groups were conducted using one-way analysis of variance (ANOVA) with Tukey's post hoc tests. The Kaplan-Meier method was used to calculate the survival rate. Values of $p < 0.05$ were considered statistically significant.

Results

RIPC Relieves ALI in Septic Rats

RIPC has been established to be a beneficial stimulation triggered by transient ischemia-reperfusion of distal tissues, which has a protective effect on heart and kidney [3, 5, 21], but the protective mechanism of RIPC in sepsis-induced ALI is still unknown. Thus, sepsis rat models

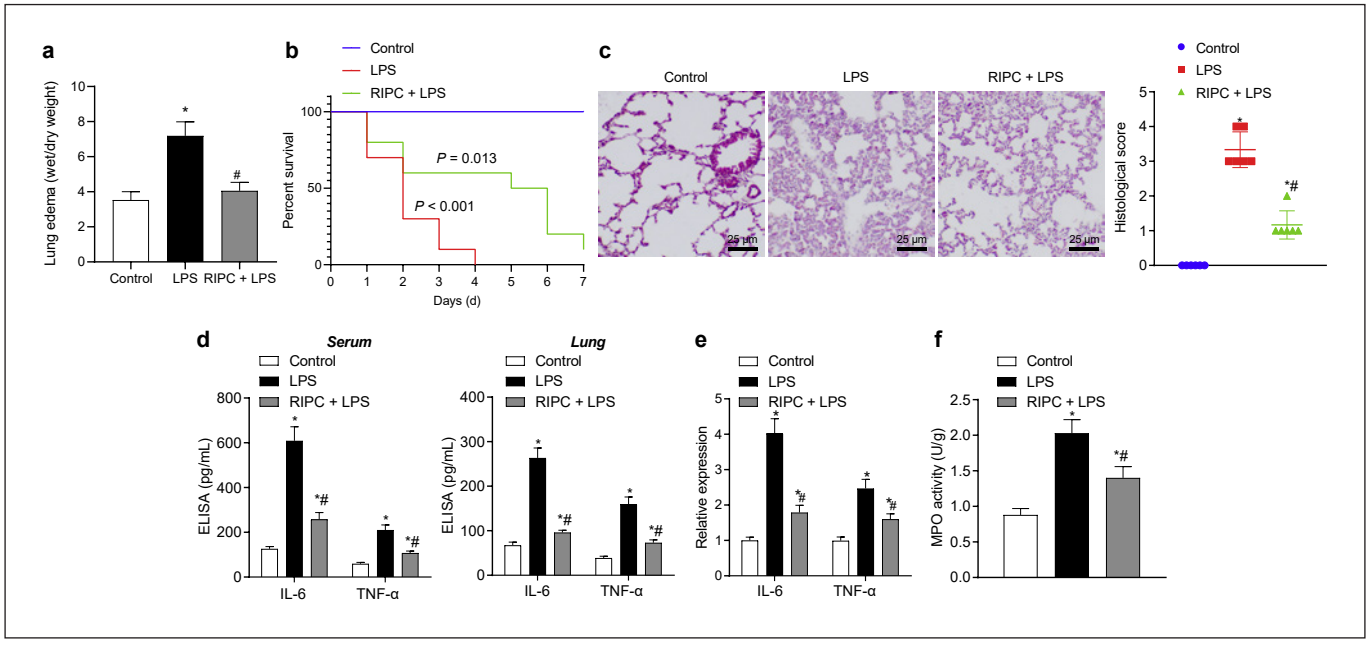

Fig. 1. RIPC alleviates LPS-induced sepsis in rats. **a** The formation of pulmonary edema in LPS-induced septic ALI rats, determined by W/D ratio. **b** Survival rate of LPS-induced septic ALI rats. **c** Morphology of lung tissues of LPS-induced septic ALI rats detected by HE staining. **d** Levels of TNF-α and IL-6 in serum and lung tissues of LPS-induced septic ALI rats measured by ELISA. **e** mRNA levels of TNF-α and IL-6 in serum and lung tissues of septic rats 6 h after LPS induction measured by RT-qPCR. **f** The infiltration of inflammatory cells into lung tissues in LPS-induced septic ALI rats detected by MPO activity. $^{*}p < 0.05$ versus rats injected with normal saline (the control group); $^{\#}p < 0.05$ versus LPS-induced septic ALI rats (the LPS group). Descriptive data are summarized as the mean ± standard deviation. Data comparison between multiple groups was conducted using the one-way ANOVA with Tukey's post hoc test. The Kaplan-Meier method was used to calculate the survival rate. $n = 6$ for rats upon each treatment. W/D ratio, wet/dry ratio.

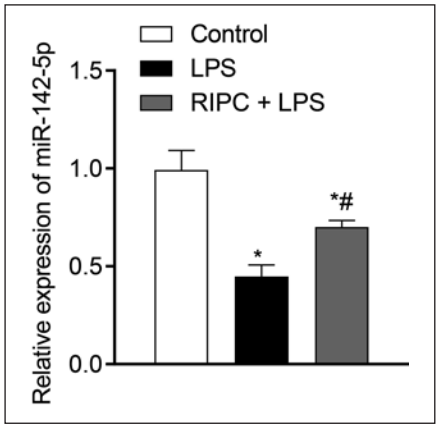

Fig. 2. miR-142-5p expression increases in lung tissues of LPS-induced septic ALI rats receiving RIPC treatment. miR-142-5p expression in lung tissues of LPS-induced septic ALI rats measured by RT-qPCR. $^{*}p < 0.05$ versus rats injected with normal saline; $^{\#}p < 0.05$ versus LPS-induced septic ALI rats. Descriptive data are summarized as the mean ± standard deviation. Data comparison among multiple groups was conducted using one-way ANOVA with Tukey's post hoc test. $n = 6$ for rats upon each treatment.

were induced by LPS to investigate the effects of RIPC on ALI in septic rats. Compared with untreated LPS-induced septic ALI rats, RIPC treatment reduced the formation of pulmonary edema (Fig. 1a). Within 7 days after RIPC treatment, RIPC increased the survival rate of LPS-induced septic ALI rats (Fig. 1b). The results of HE staining showed that RIPC could attenuate the formation of edema and neutrophil infiltration in lung tissues of septic rats after LPS induction (Fig. 1c).

It has been documented that the increases in the production of proinflammatory TNF-α and IL-6 in serum and lung tissues were markers of the inflammatory response in lungs [22, 23]. ELISA results displayed that TNF-α and IL-6 levels in serum and lung tissues increased at 6 h after LPS induction, while RIPC blocked the increase of these cytokines in serum and lung tissues in LPS-induced septic ALI rats (Fig. 1d). Meanwhile, the expression of TNF-α and IL-6 mRNA was elevated in these lung tissues, whereas the elevation was reversed following RIPC (Fig. 1e). MPO evaluation results further verified

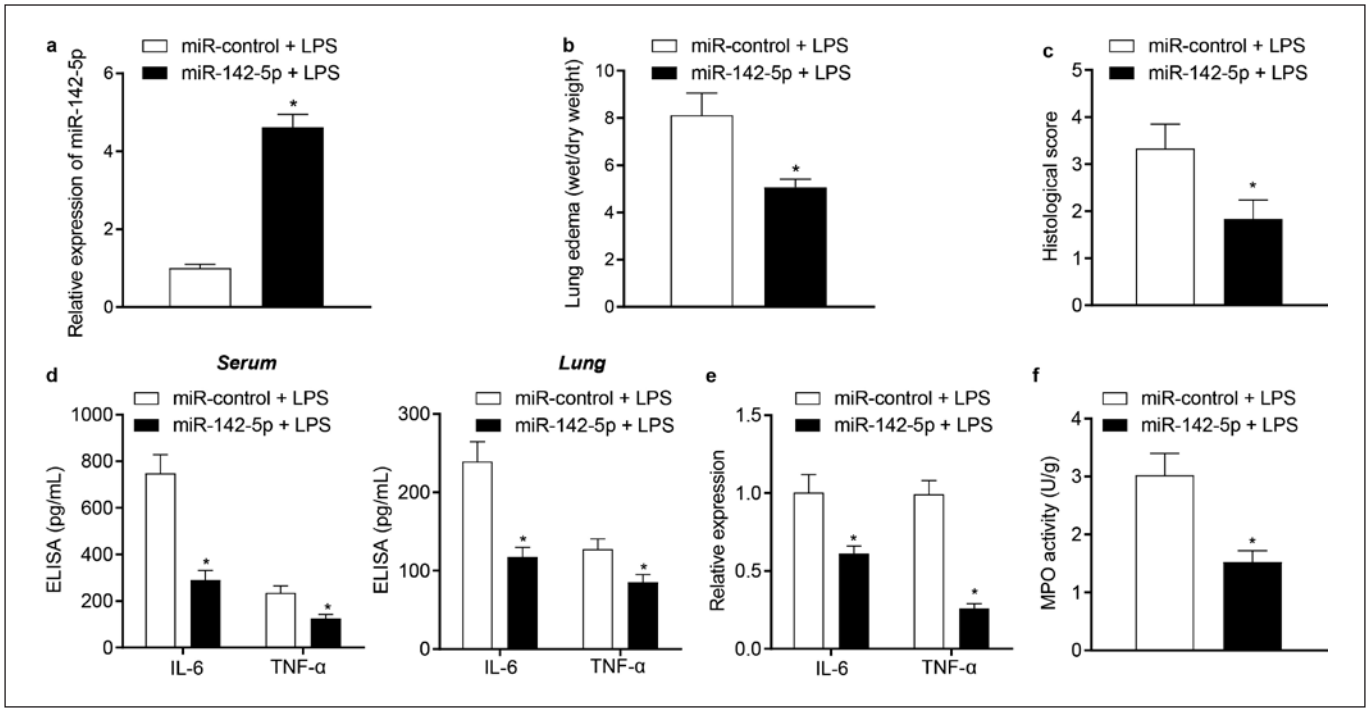

Fig. 3. miR-142-5p relieves LPS-induced ALI in septic rats. **a** miR-142-5p expression in lung tissues of rats in response to miR-NC + LPS or miR-142-5p + LPS measured by RT-qPCR. **b** The formation of pulmonary edema in lung tissues of rats in response to miR-NC + LPS or miR-142-5p + LPS determined by W/D ratio. **c** Morphology of lung tissues of rats in response to miR-NC + LPS or miR-142-5p + LPS detected by HE staining. **d** Levels of TNF-α and IL-6 in serum and lung tissues of rats in response to miR-NC + LPS or miR-142-5p + LPS measured by ELISA. **e** mRNA levels of TNF-α and IL-6 in serum and lung tissues of rats in response to miR-NC + LPS or miR-142-5p + LPS measured by RT-qPCR. **f** The infiltration of inflammatory cells into lung tissues in rats in response to miR-NC + LPS or miR-142-5p + LPS detected by MPO activity. *$p < 0.05$ versus LPS-induced septic rats injected with miR control (the miR control + LPS group). Descriptive data are summarized as the mean ± standard deviation. Data from 2 groups were compared by the unpaired *t* test. Data comparison between multiple groups was conducted using the one-way ANOVA with Tukey's post hoc test. $n = 6$ for rats upon each treatment. W/D ratio, wet/dry ratio.

that RIPC attenuated lung inflammation in septic rats (Fig. 1f). These results suggested that RIPC protected against septic ALI in LPS-challenged rats.

miR-142-5p Is Upregulated in Lung Tissues of LPS-Induced Septic ALI Rats following RIPC

Evidence exists reporting the involvement of miRNAs in inflammatory lung diseases [12, 23], The underexpression of miR-142-5p was revealed in lung tissues of LPS-induced septic ALI rats relative to control rats, whereas the rescue of miR-142-5p expression was observed in response to RIPC treatment (Fig. 2). These data suggested that RIPC elevated miR-142-5p expression in LPS-induced septic ALI.

miR-142-5p Alleviates LPS-Induced ALI in Septic Rats

To explore whether systemic administration of miR-142-5p reduced sepsis-induced ALI, miR-142-5p or miR-control was intravenously injected into the rats and they were treated with LPS 1 day after the injections. miR-142-5p expression was increased in lung tissues of rats cotreated with miR-142-5p and LPS (Fig. 3a), accompanied by a decreased formation of pulmonary edema (Fig. 3b). HE staining analysis showed that the formation of edema and neutrophil infiltration was reduced in lung tissues of rats cotreated with miR-142-5p and LPS (Fig. 3c). Moreover, ELISA results displayed that TNF-α and IL-6 levels in serum and lung tissues of rats cotreated with miR-142-5p and LPS decreased 6 h after LPS induction (Fig. 3d). RT-qPCR results revealed that mRNA levels of TNF-α and IL-6 were downregulated in lung tissues of rats cotreated with miR-142-5p and LPS (Fig. 3e). MPO evaluation further verified that miR-142-5p attenuated lung inflammation in LPS-induced septic ALI rats (Fig. 3f). It can thus be concluded that miR-142-5p attenuated ALI in LPS-induced septic rats.

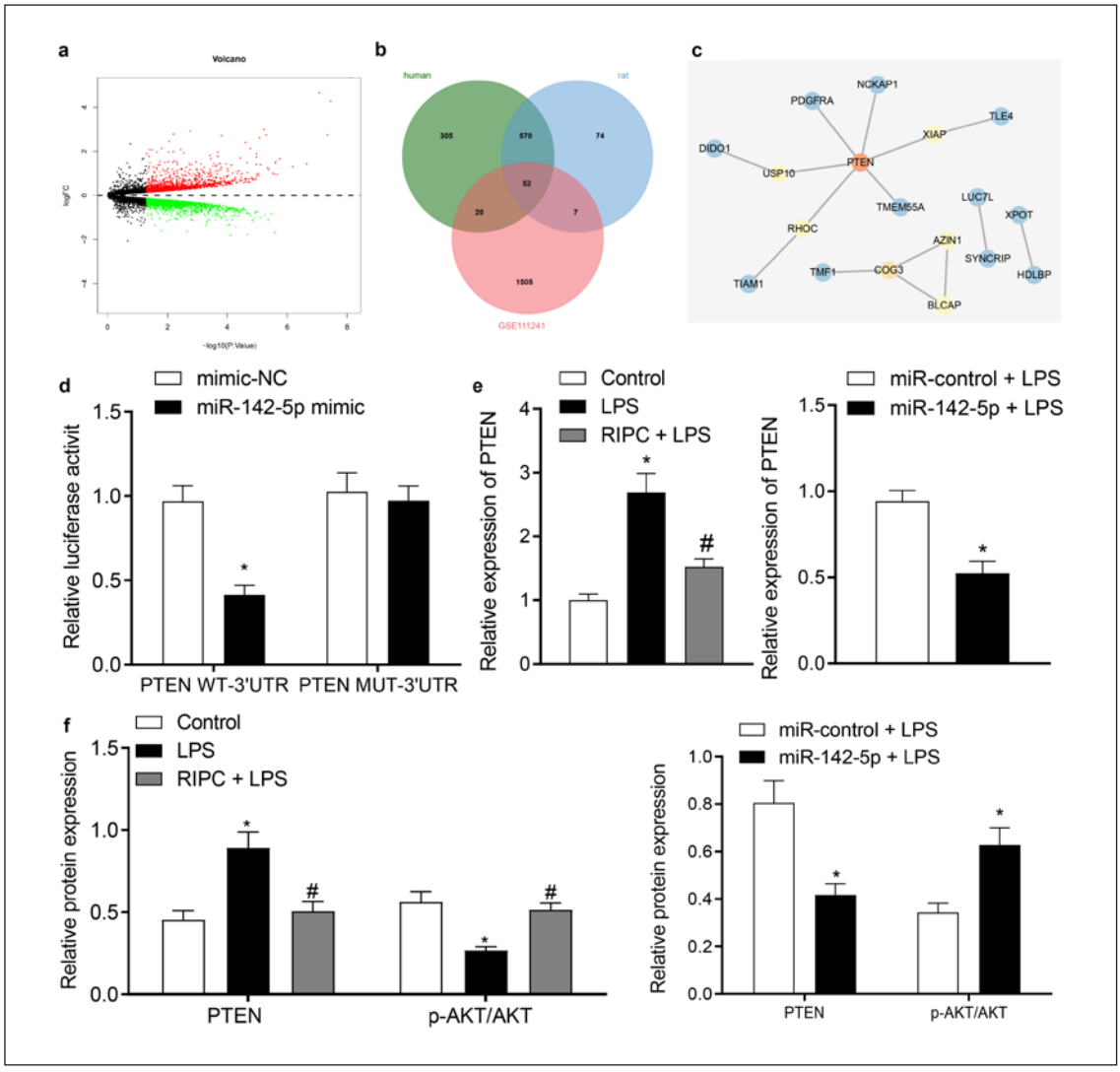

Fig. 4. miR-142-5p activates the PI3K/Akt signaling pathway by targeting PTEN. **a** Volcano map of DEGs in the GSE111241 microarray data. Green represents significantly downregulated mRNAs and red represents significantly upregulated mRNAs. **b** Venn map of hsa-miR-142-5p (green) and rno-miR-142-5p (blue) target genes and significantly upregulated genes (red) in the GSE111241 microarray data. **c** The interaction network of 52 genes analyzed using the STRING database (https://string-db.org/). Brighter color of the circle reflected a higher degree value of the gene. **d** There are seven base pairs of PTEN 3′-UTR complementary to miR-142-5p (the upper part), and luciferase activity was detected by the dual-luciferase reporter gene assay (the lower part). **e** PTEN mRNA level and miR-142-5p expression in lung tissues of rats in response to LPS alone or combined with RIPC/miR-142-5p measured by RT-qPCR ($n = 6$). **f** Protein levels of PTEN and p-AKT/AKT in lung tissues of rats in response to LPS alone or combined with RIPC/miR-142-5p measured by the Western blot analysis ($n = 6$). $^{*}p < 0.05$ versus control rats or LPS-induced septic rats injected with miR control; $^{\#}p < 0.05$ versus LPS-induced septic ALI rats. Descriptive data are depicted as the mean ± standard deviation. Data from 2 groups were compared by the unpaired *t* test. Data comparisons between multiple groups were conducted by one-way ANOVA with Tukey's post hoc test. UTR, untranslated region; WT, wild type; MUT, mutant.

miR-142-5p Targets PTEN to Activate the PI3K/Akt Signaling Pathway

The TargetScan database was utilized to predict miR-142-5p target genes, and the sepsis-induced ALI-related mRNA dataset GSE111241 was subjected to the differential analysis (Fig. 4a). Following Venn diagram analysis of the predicted target genes of miR-142-5p and upregulated mRNAs in the GSE111241 dataset, 52 genes were found at the intersection (Fig. 4b). In order to identify the target genes, the interactions between these 52 genes were

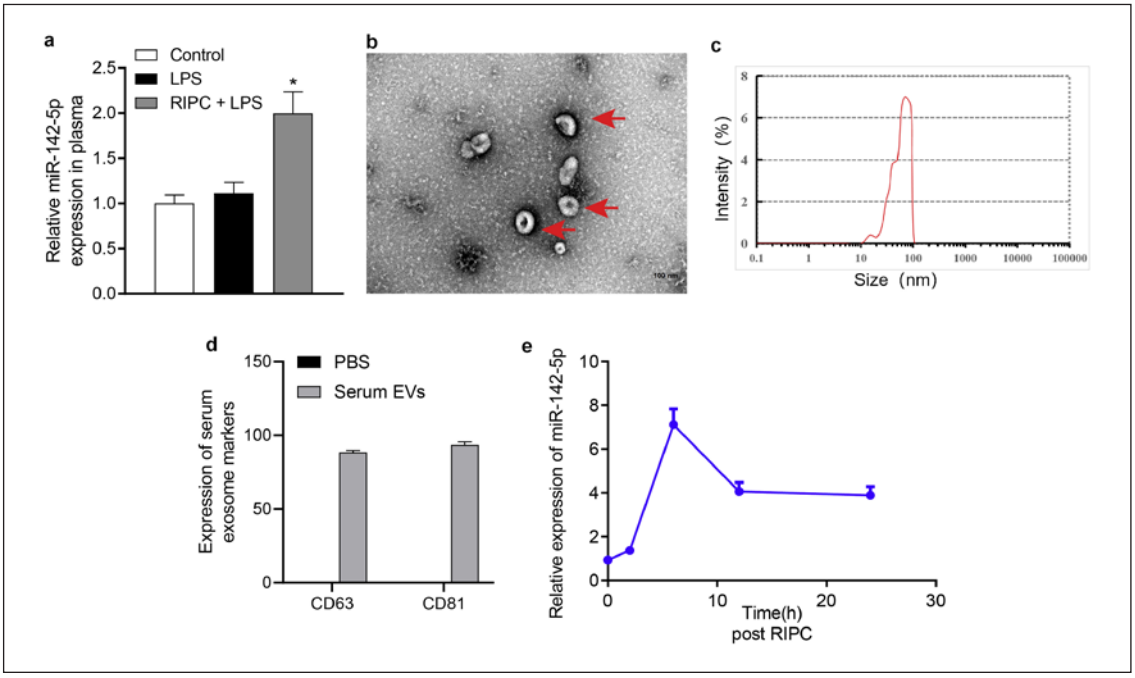

Fig. 5. miR-142-5p is upregulated in serum-derived EVs of LPS-induced septic ALI rats following RIPC. **a** miR-142-5p expression in plasma of LPS-induced septic ALI rats following RIPC, determined by RT-qPCR ($n = 6$). **b** EVs in serum of LPS-induced septic ALI rats following RIPC, observed by TEM (EVs are indicated by arrows). **c** The size and concentration of EVs from serum of rats analyzed by NTA ($n = 3$). **d** Serum-derived EV markers, CD63 and CD81, detected by flow cytometry ($n = 3$) with PBS as the control. **e** miR-142-5p expression in serum-derived EVs of LPS-induced septic ALI rats at different time points after RIPC treatment ($n = 3$). *$p < 0.05$ versus LPS-induced septic ALI rats. Descriptive data are summarized as the mean ± standard deviation. Data comparison for multiple groups was conducted using one-way ANOVA with Tukey's post hoc test. TEM, transmission electron microscope.

analyzed by using the STRING database, and PTEN was found to be a hub gene (Fig. 4c). A dual-luciferase reporter gene assay data revealed that miR-142-5p could target PTEN (Fig. 4d). In vivo, as compared to the rats injected with normal saline, PTEN mRNA and protein levels increased and the p-AKT/AKT protein level decreased in lung tissues of LPS-induced septic ALI rats. Relative to LPS-induced septic ALI rats, the PTEN mRNA and protein levels were reduced and p-AKT/AKT protein level was elevated in the lung tissues of LPS-induced septic ALI rats following RIPC. Compared to rats injected with miR-control and LPS, miR-142-5p expression and p-AKT/AKT protein level were increased, whereas PTEN mRNA and protein levels were decreased in rats injected with miR-142-5p and LPS (Fig. 4e, f; online suppl. Fig. S1). Collectively, these results unveiled that miR-142-5p activated the PI3K/Akt signaling pathway by inhibiting PTEN.

miR-142-5p Expression Elevates in Serum-Derived EVs of LPS-Induced Septic ALI Rats following RIPC

It has been found that RIPC treatment could upregulate miR-142-5p in the lung tissues of rats. We speculated that RIPC may release miR-142-5p into the blood, which acted as a humoral lung protective factor. Thus, the effect of RIPC on circulating miR-142-5p expression was investigated. Relative to rats injected with normal saline, miR-142-5p expression exhibited no difference in the plasma of LPS-induced septic ALI rats, while it was 2-folds higher in the plasma of LPS-induced septic ALI rats following RIPC than those without RIPC treatment (Fig. 5a). Since EVs are important carriers of circulating miRNA, the response of EVs to RIPC was explored. Transmission electron microscope data displayed that EVs extracted from rat serum had a double-membrane structure, similarly in a circle or an oval shape with complete membrane (Fig. 5b). In addition, nanoparticle tracking analysis indicated that the diameter of EVs was between 25 nm and 150 nm, where 90.15 nm was average (Fig. 5c). The pres-

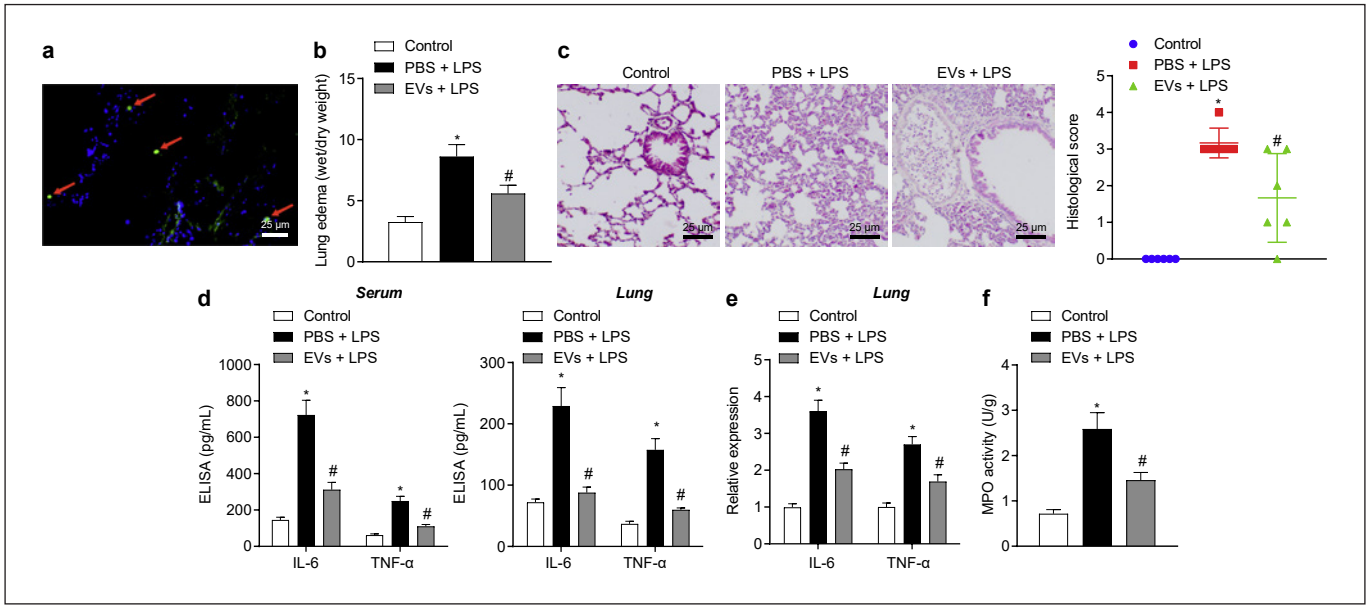

Fig. 6. Serum-derived EVs relieve LPS-induced ALI in sepsis following RIPC. Rats were injected with LPS and EVs. **a** The distribution of PKH67-labeled EVs in lung tissues observed by immunofluorescence (PKH67-conjugated EVs are indicated by red arrows). **b** The formation of pulmonary edema in lung tissues of rats determined by the W/D ratio. **c** Representative images and quantitative analysis of lung injury detected by HE staining. **d** Levels of TNF-α and IL-6 in serum and lung tissues of rats measured by ELISA. **e** mRNA levels of TNF-α and IL-6 in serum and lung tissues of rats at 6 h after LPS induction measured by RT-qPCR. **f** The infiltration of inflammatory cells into lung tissues in rats detected by MPO activity. $^{*}p < 0.05$ versus rats injected with rats injected with normal saline; $^{\#}p < 0.05$ versus rats injected with PBS + LPS. Descriptive data are summarized as the mean ± standard deviation. Data comparisons for multiple groups were conducted using one-way ANOVA with Tukey's post hoc test. $n = 6$ for rats in each treatment group. W/D ratio, wet/dry ratio.

ence of EV markers CD63 and CD81 was identified with flow cytometry (Fig. 5d). Furthermore, miR-142-5p expression in EVs at different time points (0, 2, 6, 12, and 24 h) after RIPC treatment was determined. The level of EVs-miR-142-5p in the serum of rats was found upregulated 2 h after RIPC treatment, which remained stable up to 24 h (Fig. 5e). These findings suggested that EVs-miR-142-5p expression was elevated in the serum of LPS-induced septic ALI rats following RIPC.

Serum-Derived EVs Alleviate ALI in LPS-Induced Septic Rats following RIPC

To verify whether the protective effect of RIPC on sepsis-induced ALI is mediated by EVs, the distribution of serum-derived EVs in the lung tissue of rats with sepsis-induced ALI after RIPC treatment was determined. Serum-derived EVs labeled with PKH67 were intravenously injected into sepsis-induced ALI rats. After 24 h, frozen sections displayed that the EVs labeled with PKH67 were carried into the lung parenchyma (Fig. 6a). In contrast to PBS-treated rats, the formation of pulmonary edema was enhanced in rats injected with PBS + LPS, whereas additional injection of EVs negated the enhancement (Fig. 6b). As depicted in HE staining, relative to PBS-treated rats, the formation of edema and neutrophil infiltration was greater in the lung tissues of rats injected with PBS + LPS. Compared with the rats injected with PBS + LPS, the formation of edema and neutrophil infiltration was decreased in the lung tissues of rats injected with EVs + LPS (Fig. 6c). ELISA and RT-qPCR data displayed that the levels of TNF-α and IL-6 increased in serum and lung tissues of rats treated with PBS + LPS relative to those in control rats, whereas these increases were reversed in response to injection of EVs (Fig. 6d, e). MPO evaluation further verified that as compared to rats injected with normal saline, lung inflammation was strengthened in rats injected with PBS + LPS. As compared to the rats injected with PBS + LPS, lung inflammation was attenuated in rats injected with EVs + LPS (Fig. 6f). These lines of evidence led to a conclusion that serum-derived EVs attenuated ALI in LPS-induced sepsis following RIPC in a rat model.

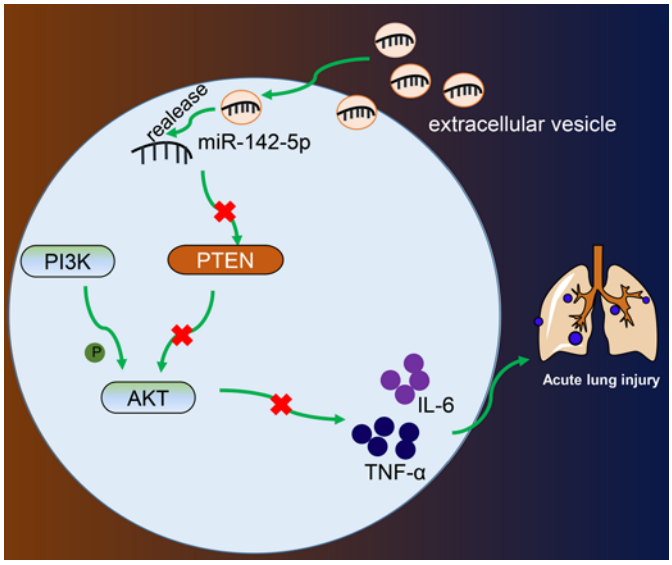

Fig. 7. A schematic diagram showing that serum-derived EVs-loaded miR-142-5p can mediate the PTEN/PI3K/Akt axis to alleviate ALI in septic rats.

Discussion

ALI is a frequent fatal complication of sepsis due to high pulmonary susceptibility [24]. In recent years, RIPC has been proved to protect against lung injury [25]. Here, we provided evidence demonstrating that miR-142-5p shuttled by serum-derived EVs exerted inhibitory effects on LPS-induced septic ALI following RIPC via downregulation of PTEN and activation of the PI3K/Akt axis (Fig. 7).

Initial findings revealed that RIPC reduced the formation of pulmonary edema, neutrophil infiltration, and TNF-α and IL-6 levels, thus alleviating ALI in LPS-induced septic rats. Notably, ALI can induce the release of bacterial endotoxins such as LPS, which can trigger the inflammatory response, leading to lung injury characterized by inflammatory leukocyte infiltration [26]. It is known that the release of inflammatory mediators and the promotion of apoptosis are implicated in the progression of sepsis-induced ALI [27]. Mounting evidence has confirmed that RIPC can inhibit the pulmonary inflammatory reaction by reducing TNF-α and IL-6 levels, neutrophil activation, and infiltration and thus protect against lung injury [28, 29]. A prior study has also revealed that RIPC can alleviate systemic inflammation induced by LPS to increase survival rates in septic mice [6]. These reports support the present finding that RIPC attenuated ALI in LPS-induced septic rats.

In addition, the findings of the current study demonstrated that serum-derived EVs alleviated ALI in LPS-induced septic rats following RIPC. Existing reports have noted the beneficial effects of EVs on attenuating inflammatory lung injury in both ALI and sepsis [7, 30]. Zhou et al. [31] have indicated that endothelial progenitor cell-derived exosomes contribute to a reduction in the permeability, inflammation, MPO activity, and pulmonary edema to protect against lung injury. Moreover, exosomes carrying miRNAs suppress inflammatory responses to mitigate LPS-induced acute septic lung injury [32]. In accordance, this study proved that miR-142-5p shuttled by serum-derived EVs relieved LPS-induced septic ALI. Substantial evidence suggests that miRNAs act as significant mediators in immune system development and thus are implicated in certain inflammatory lung diseases, including ALI [9, 11]. Underexpression of miR-490-3p occurred in LPS-induced ALI rats, and restoration of miR-490-3p represses LPS-induced lung epithelial cell injury [10]. Upregulated miR-26a-5p has been found to attenuate LPS-induced inflammatory responses in ALI mice by reducing levels of proinflammatory cytokines and MDA and MPO activity in LPS-induced A549 cells [33]. miR-142-5p expression reportedly decreases in sepsis [14]. A recent study has exhibited that miR-142-5p is poorly expressed in nonsmall cell lung cancer tissues, and restored miR-142-5p in tumor cells can inhibit cell proliferation and metastasis while inducing cell apoptosis [13, 34].

Furthermore, miR-142-5p could target PTEN to activate the PI3K/Akt signaling pathway in sepsis-induced ALI. In agreement, Wan et al. [35] have also demonstrated that overexpressed miR-142-5p inhibits PTEN protein expression. It is interesting to note that PTEN induces inflammatory responses in sepsis-induced ALI [18]. PTEN, serving as a negative regulator of the PI3K/Akt signaling pathway, repressed the inflammatory response in ALI [36, 37]. PTEN activation stimulates inflammatory responses by suppressing the PI3K signaling pathway in sepsis-induced lung injury [17]. The protective effects of the PI3K/Akt signaling pathway on pulmonary inflammation in LPS-induced ALI have been investigated [38]. A previous study has also confirmed that the PI3K/Akt signaling pathway is linked to the reduction in proinflammatory cytokine, thereby attenuating pulmonary inflammation in LPS-induced ALI [24]. These findings support our notion that miR-142-5p shuttled by serum-secreted EVs attenuated ALI in sepsis by inhibiting PTEN and activation of the PI3K/Akt signaling pathway.

To sum up, our study demonstrated that the transfer of miR-142-5p via serum-derived EVs altered the PI3K/

Akt expression, by negatively regulating PTEN, all of which leads to the alleviation of LPS-induced ALI in sepsis following RIPC. At present, there are studies on the relationship between ALI and PTEN, such as lncRNA [39] and single cell-derived EVs, such as mesenchymal stem cell EVs, on the PTEN signaling pathway in ALI [40]. The highlight of this study is to start from the miRNA carried by serum EVs for the first time to study whether EVs carry miRNA to regulate PTEN signaling pathway, so as to reduce ALI in sepsis. Unlike single-cell EVs, serum-derived EVs include the EVs of many cells in the body, and it can better reflect the value of studying the relationship between EV-encapsulated miRNA and the PTEN signaling pathway in ALI in sepsis.

Statement of Ethics

The animal experimental protocols were approved by the Institutional Animal Care and Use Committee of Henan Provincial People's Hospital (Approval No. 2019039). All animal experiments were performed in strict accordance with the Guide for the Care and Use of Laboratory Animals.

Conflict of Interest Statement

The authors declare that they have no competing interests.

Funding Sources

No funding was received for this study.

Author Contributions

Wenliang Zhu conceived and designed research. Xiaopei Huang performed experiments. Shi Qiu interpreted results of experiments. Lingxiao Feng analyzed data and prepared figures. Yue Wu drafted the paper. Huanzhang Shao edited and revised the manuscript. All authors read and approved the final version of the manuscript.

Data Availability Statement

The datasets generated during and/or analyzed during the current study are available from the corresponding author on reasonable request.

References

1 Poston JT, Koyner JL. Sepsis associated acute kidney injury. BMJ. 2019;364:k4891.
2 Aziz M, Ode Y, Zhou M, Ochani M, Holodick NE, Rothstein TL, et al. B-1a cells protect mice from sepsis-induced acute lung injury. Mol Med. 2018;24:26.
3 Pan T, Jia P, Chen N, Fang Y, Liang Y, Guo M, et al. Delayed remote ischemic preconditioning confers renoprotection against septic acute kidney injury via exosomal miR-21. Theranostics. 2019;9:405–23.
4 Zarbock A, Schmidt C, Van Aken H, Wempe C, Martens S, Zahn PK, et al. Effect of remote ischemic preconditioning on kidney injury among high-risk patients undergoing cardiac surgery: a randomized clinical trial. JAMA. 2015;313:2133–41.
5 Yamaguchi T, Izumi Y, Nakamura Y, Yamazaki T, Shiota M, Sano S, et al. Repeated remote ischemic conditioning attenuates left ventricular remodeling via exosome-mediated intercellular communication on chronic heart failure after myocardial infarction. Int J Cardiol. 2015;178:239–46.
6 Kim YH, Kim YS, Kim BH, Lee KS, Park HS, Lim CH. Remote ischemic preconditioning ameliorates indirect acute lung injury by modulating phosphorylation of IκBα in mice. J Int Med Res. 2019;47:936–50.
7 Mahida RY, Matsumoto S, Matthay MA. Extracellular vesicles: a new frontier for research in acute respiratory distress syndrome. Am J Respir Cell Mol Biol. 2020;63:15–24.
8 Wang J, Huang R, Xu Q, Zheng G, Qiu G, Ge M, et al. Mesenchymal stem cell-derived extracellular vesicles alleviate acute lung injury via transfer of miR-27a-3p. Crit Care Med. 2020;48:e599–610.
9 Fu L, Zhu P, Qi S, Li C, Zhao K. MicroRNA-92a antagonism attenuates lipopolysaccharide (LPS)-induced pulmonary inflammation and injury in mice through suppressing the PTEN/AKT/NF-kappaB signaling pathway. Biomed Pharmacother. 2018;107:703–11.
10 Yang G, Zhao Y. MicroRNA-490-3p inhibits inflammatory responses in LPS-induced acute lung injury of neonatal rats by suppressing the IRAK1/TRAF6 pathway. Exp Ther Med. 2021;21(2):152.
11 Suo T, Chen GZ, Huang Y, Zhao KC, Wang T, Hu K. miRNA-1246 suppresses acute lung injury-induced inflammation and apoptosis via the NF-κB and Wnt/β-catenin signal pathways. Biomed Pharmacother. 2018;108:783–91.
12 Wang Z, Yan J, Yang F, Wang D, Lu Y, Liu L. MicroRNA-326 prevents sepsis-induced acute lung injury via targeting TLR4. Free Radic Res. 2020;54:408–18.
13 Zhu W, Wang JP, Meng QZ, Zhu F, Hao XF. miR-142-5p reverses the resistance to gefitinib through targeting HOXD8 in lung cancer cells. Eur Rev Med Pharmacol Sci. 2020;24:4306–13.
14 Ge QM, Huang CM, Zhu XY, Bian F, Pan SM. Differentially expressed miRNAs in sepsis-induced acute kidney injury target oxidative stress and mitochondrial dysfunction pathways. PLoS One. 2017;12:e0173292.
15 Lou Z, Peng Z, Wang B, Li X, Li X, Zhang X. miR-142-5p promotes the osteoclast differentiation of bone marrow-derived macrophages via PTEN/PI3K/AKT/FoxO1 pathway. J Bone Miner Metab. 2019;37:815–24.
16 Wan X, Helman LJ. Levels of PTEN protein modulate Akt phosphorylation on serine 473, but not on threonine 308, in IGF-II-overexpressing rhabdomyosarcomas cells. Oncogene. 2003;22:8205–11.
17 Zhou M, Fang H, Du M, Li C, Tang R, Liu H, et al. The modulation of regulatory T cells via HMGB1/PTEN/beta-cenin axis in LPS induced acute lung injury. Front Immunol. 2019;10:1612.
18 Liu L, Chen J, Zhang X, Cui X, Qiao N, Zhang Y, et al. The protective effect of PPARgamma in sepsis-induced acute lung injury via inhibiting PTEN/beta-catenin pathway. Biosci Rep. 2020;40:BSR20192639.
19 Varkouhi AK, Jerkic M, Ormesher L, Gagnon S, Goyal S, Rabani R, et al. Extracellular vesicles from interferon-gamma-primed human umbilical cord mesenchymal stromal cells reduce Escherichia coli-induced acute lung injury in rats. Anesthesiology. 2019;130:778–90.

20 Zhu YG, Feng XM, Abbott J, Fang XH, Hao Q, Monsel A, et al. Human mesenchymal stem cell microvesicles for treatment of escherichia coli endotoxin-induced acute lung injury in mice. Stem Cells. 2014;32:116–25.
21 Li J, Rohailla S, Gelber N, Rutka J, Sabah N, Gladstone RA, et al. MicroRNA-144 is a circulating effector of remote ischemic preconditioning. Basic Res Cardiol. 2014;109:423.
22 Li H, Hao Y, Yang LL, Wang XY, Li XY, Bhandari S, et al. MCTR1 alleviates lipopolysaccharide-induced acute lung injury by protecting lung endothelial glycocalyx. J Cell Physiol. 2020;235:7283–94.
23 Lomas-Neira J, Venet F, Chung CS, Thakkar R, Heffernan D, Ayala A. Neutrophil-endothelial interactions mediate angiopoietin-2-associated pulmonary endothelial cell dysfunction in indirect acute lung injury in mice. Am J Respir Cell Mol Biol. 2014;50:193–200.
24 Li R, Ren T, Zeng J. Mitochondrial coenzyme Q protects sepsis-induced acute lung injury by activating PI3K/Akt/GSK-3β/mTOR pathway in rats. Biomed Res Int. 2019;2019:5240898.
25 Chen K, Xu Z, Liu Y, Wang Z, Li Y, Xu X, et al. Irisin protects mitochondria function during pulmonary ischemia/reperfusion injury. Sci Transl Med. 2017;9:eaao6298.
26 Huang CY, Deng JS, Huang WC, Jiang WP, Huang GJ. Attenuation of lipopolysaccharide-induced acute lung injury by hispolon in mice, through regulating the TLR4/PI3K/Akt/mTOR and Keap1/Nrf2/HO-1 pathways, and suppressing oxidative stress-mediated er stress-induced apoptosis and autophagy. Nutrients. 2020;12:1742.
27 Qiu N, Xu X, He Y. LncRNA TUG1 alleviates sepsis-induced acute lung injury by targeting miR-34b-5p/GAB1. BMC Pulm Med. 2020;20:49.
28 Zheng L, Han R, Tao L, Yu Q, Li J, Gao C, et al. Effects of remote ischemic preconditioning on prognosis in patients with lung injury: a meta-analysis. J Clin Anesth. 2020;63:109795.
29 Camara-Lemarroy CR. Remote ischemic preconditioning as prevention of transfusion-related acute lung injury. Med Hypotheses. 2014;83:273–5.
30 Liu A, Zhang X, He H, Zhou L, Naito Y, Sugita S, et al. Therapeutic potential of mesenchymal stem/stromal cell-derived secretome and vesicles for lung injury and disease. Expert Opin Biol Ther. 2020;20:125–40.
31 Zhou Y, Li P, Goodwin AJ, Cook JA, Halushka PV, Chang E, et al. Exosomes from endothelial progenitor cells improve outcomes of the lipopolysaccharide-induced acute lung injury. Crit Care. 2019;23:44.
32 Yuan Z, Bedi B, Sadikot RT. Bronchoalveolar lavage exosomes in lipopolysaccharide-induced septic lung injury. J Vis Exp. 2018;23:57737.
33 Li H, Yang T, Fei Z. miR-26a-5p alleviates lipopolysaccharide-induced acute lung injury by targeting the connective tissue growth factor. Mol Med Rep. 2021;23:1.
34 Jiang Q, Xing W, Cheng J, Yu Y. Knockdown of lncRNA XIST suppresses cell tumorigenicity in human non-small cell lung cancer by regulating miR-142-5p/PAX6 axis. Onco Targets Ther. 2020;13:4919–29.
35 Wan J, Ling X, Peng B, Ding G. miR-142-5p regulates CD4+ T cells in human non-small cell lung cancer through PD-L1 expression via the PTEN pathway. Oncol Rep. 2018;40:272–82.
36 Kalantari P, Harandi OF, Agarwal S, Rus F, Kurt-Jones EA, Fitzgerald KA, et al. miR-718 represses proinflammatory cytokine production through targeting phosphatase and tensin homolog (PTEN). J Biol Chem. 2017;292:5634–44.
37 Qin S, Wang H, Liu G, Mei H, Chen M. miR-21-5p ameliorates hyperoxic acute lung injury and decreases apoptosis of AEC II cells via PTEN/AKT signaling in rats. Mol Med Rep. 2019;20:4953–62.
38 Meng L, Li L, Lu S, Li K, Su Z, Wang Y, et al. The protective effect of dexmedetomidine on LPS-induced acute lung injury through the HMGB1-mediated TLR4/NF-kappaB and PI3K/Akt/mTOR pathways. Mol Immunol. 2018;94:7–17.
39 Lv X, Zhang XY, Zhang Q, Nie YJ, Luo GH, Fan X, et al. lncRNA NEAT1 aggravates sepsis-induced lung injury by regulating the miR-27a/PTEN axis. Lab Invest. 2021;101:1371–81.
40 Wu Y, Li J, Yuan R, Deng Z, Wu X. Bone marrow mesenchymal stem cell-derived exosomes alleviate hyperoxia-induced lung injury via the manipulation of microRNA-425. Arch Biochem Biophys. 2021;697:108712.